A NEW SINGULARITY INDEX

Gautam S. Muralidhar, Alan C. Bovik, and Mia K. Markey

The University of Texas at Austin
Austin, TX, USA

ABSTRACT

We propose a new ratio index for the detection of impulse-like singularities in signals of arbitrary dimensionality. We show that the new singularity index responds strongly to singularities that are like impulses or smoothed impulses in cross section. For example, it responds strongly to curvilinear masses (ridges) in images, while responding minimally to edge-like singularities. The ratio index employs directional derivatives of gaussians, which makes the index naturally scalable.

Index Terms— Singularities, impulses, singularity detection, image curves.

1. INTRODUCTION

Detection of singularities in images is a widely studied problem in computer vision and image analysis, since singularities correspond to luminance discontinuities and provide evidence of object contours and surface boundaries. Two types of singularities are often encountered: 1) edge (jump) singularities, and 2) impulse-like singularities such as curvilinear ridges in images. Impulses or curve-like singularities often arise from curvilinear objects that exist at fine scales. Locating curve-like singularities is important in many applications such as the detection of blood vessels and cancers in human anatomy, filaments in images of biological specimens and astronomical bodies, and roads and river deltas in satellite images [1].

Many approaches have been proposed for detecting and localizing singularities in images. The history of edge detection dating from Roberts [2] was greatly advanced by Marr and Hildreth [3] and Canny [4] who employed smoothed Laplacian and gradient operators to detect jump discontinuities. Mallat and Hwang [5] studied singularity detection in the context of wavelet theory. They characterized the Lipschitz regularity of the wavelet transform modulus extrema across scales and showed that the Lipschitz exponent could be used to reveal whether the signal varied smoothly, or whether there was an edge, or an impulse like singularity [5]. Lindeberg [6] and Steger [7] presented a general scale-space framework for detecting edges and ridges.

Here we present a new ratio index for the detection of impulse singularities in images. The new index is inspired by the conditions put forth by Lindeberg [6] and Steger [7], by
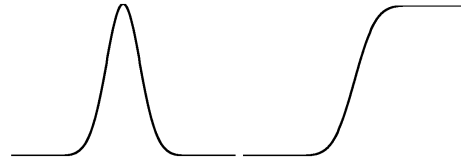

Fig. 1. 1-D impulse (left) and edge (right) profiles.

Canny's approach to directional edge detection [4], and by an energy operator developed by Teager and studied in detail by Kaiser [8]. We show analytically and experimentally that the singularity index responds strongly to impulse- or ridge-like curves in images, while responding minimally to edges.

2. PROPOSED SINGULARITY INDEX

We first consider the new singularity index in 1-D. Let $f(x), x \in R$ be a 1-D signal. Let $f'(x)$ and $f''(x)$ denote first and second order derivatives, respectively. Then define the ratio index

$$\psi[f(x)] = \frac{|f(x)f''(x)| + C_1}{|f'(x)|^2 + C_2} \qquad (1)$$

where C_1, $C_2 \in R$. Clearly $\psi[f(x)]$ is a dimensionless quantity. Ignoring the constants for a moment, the index ψ is designed to respond strongly to impulse-like singularities, where the twice-derivative is large, but to respond weakly to step-like singularities, where the once-derivative is large. Where the once-derivative is small, the denominator should have little effect. This suggests the nominal values $C_1 = 0$ and $C_2 = 1$ although other criteria such as noise might promote other choices of these constants. For simplicity of discussion, we assume the nominal values, hence

$$\psi[f(x)] = \frac{|f(x)f''(x)|}{1 + |f'(x)|^2} \qquad (2)$$

Next we study the response of ψ on 1-D impulse and edge profiles.

2.1. 1-D impulse profile

Model a smoothed 1-D impulse as a gaussian of height $K > 0$ and scale σ (see Fig. 1, left):

$$f(x) = Ke^{\frac{-x^2}{2\sigma^2}} \tag{3}$$

The first and second derivatives are:

$$f'(x) = \frac{-Kx}{\sigma^2}e^{\frac{-x^2}{2\sigma^2}} \tag{4}$$

$$f''(x) = \frac{K}{\sigma^2}\left(\frac{x^2}{\sigma^2} - 1\right)e^{\frac{-x^2}{2\sigma^2}} \tag{5}$$

Substituting (3)-(5) into (2) yields

$$\psi[f(x)] = \frac{\left(\left|\frac{K^2}{\sigma^2}\right|\left|\frac{x^2}{\sigma^2} - 1\right|e^{\frac{-x^2}{\sigma^2}}\right)}{1 + \left(\left|\frac{Kx}{\sigma^2}\right|^2 e^{\frac{-x^2}{\sigma^2}}\right)} \tag{6}$$

At $x = 0$,

$$\psi[f(0)] = \left|\frac{K^2}{\sigma^2}\right| \tag{7}$$

Clearly as the height K of the impulse increases, or as the scale σ of the impulse decreases, $\psi[f(0)]$ increases, which is desired. The singularity index favors sharp, high-magnitude impulses. In the limit $\sigma \to \infty$, or $x \to \infty$, $\psi \to 0$. Thus the index vanishes with increased smoothness of, or distance from the impulse. The singularity index responds to both positive going and negative going impulses, although the polarity could easily be retained. Note that Lindeberg [6] and Steger [7] in their scale-space ridge detection work proposed that the first order derivative in the direction of the maximum eigen value of the Hessian matrix of the signal be 0, while the second order derivative in the same direction be non zero. The singularity index ψ naturally embodies these conditions tying the first order and second order derivatives together in a simple and elegant way to yield a dimensionless quantity.

2.2. 1-D edge profile

Model a 1-D edge profile as a step $u(x)$ of height $K > 0$ smoothed by a gaussian $g_\sigma(x)$ (see Fig. 1, right):

$$f(x) = g_\sigma(x) * u(x) = \frac{K}{\sqrt{2\pi}\sigma}\int_{-\infty}^{x} e^{\frac{-t^2}{2\sigma^2}}\,\mathrm{d}t \tag{8}$$

The derivatives of $f(x)$ are:

$$f'(x) = \frac{K}{\sqrt{2\pi}\sigma}e^{\frac{-x^2}{2\sigma^2}} \tag{9}$$

$$f''(x) = \frac{-Kx}{\sqrt{2\pi}\sigma^3}e^{\frac{-x^2}{2\sigma^2}} \tag{10}$$

Substituting (8)-(10) into (2) yields

$$\psi[f(x)] = \frac{\left(\left|\frac{K^2}{2\pi\sigma^4}\right||x|\left(\int_{-\infty}^{x} e^{\frac{-x^2}{2\sigma^2}}\,\mathrm{d}x\right)\left(e^{\frac{-x^2}{2\sigma^2}}\right)\right)}{1 + \left(\left|\frac{K}{\sqrt{2\pi}\sigma}\right|^2 e^{\frac{-x^2}{\sigma^2}}\right)} \tag{11}$$

At $x = 0$, the index vanishes:

$$\psi[f(0)] = 0 \tag{12}$$

In the neighborhood of the edge, the index decreases with K, which is desired. Finally, as $x \to \infty$, $\psi[f(x)] \to 0$; in the absence of other stimuli, the index vanishes away from the edge. Note that Koller *et al.* [1] developed a line detector that responds only to lines and not edges. Their method combines the edge responses of two neighboring shifted first order directional gaussian derivatives.

2.3. Comments on the 1-D singularity index

We defined the index ψ in (1) as operating directly on the signal f without additional smoothing or control of scale. More generally, define a smoothed singularity index

$$\psi_\sigma[f(x)] = \frac{|g_\sigma * f(x)||g_\sigma'' * f(x)|}{1 + |g_\sigma' * f(x)|^2} \tag{13}$$

to control scale directly. Here, g_σ is a smoothing filter such as a gaussian, and g_σ' and g_σ'' are its first and second derivatives. This also stabilizes derivative computations and reduces the influence of noise.

The index ψ in (1) with $C_1 = C_2 = 0$ is closely related to the Teager-Kaiser energy operator $f'(x)^2 - f(x)f''(x)$ [8], with the difference being replaced by an absolute ratio. In prior work, we used the Teager-Kaiser operator for a different purpose - demodulating AM-FM signals [9] [10], but we observed the operator to also be strongly responsive to singularities.

2.4. 2-D Singularity Index

The singularity index (1) is easily extended to 2-D. Let $f(x, y), R^2 \to R$ be the 2-D image luminance function, ∇^2 be the 2-D Laplacian $\nabla^2 f(x, y) = \left(\frac{\partial^2 f(x,y)}{\partial x^2} + \frac{\partial^2 f(x,y)}{\partial y^2}\right)$ and ∇ be the 2-D gradient $\nabla f(x, y) = \left(\frac{\partial f(x,y)}{\partial x}, \frac{\partial f(x,y)}{\partial y}\right)^T$. Then the 2-D singularity index is defined

$$\psi[f(x, y)] = \frac{|f(x, y)\nabla^2 f(x, y)| + C_1}{|\nabla f(x, y)|^2 + C_2} \tag{14}$$

We will again assume nominal values for the constants, hence

$$\psi[f(x, y)] = \frac{|f(x, y)\nabla^2 f(x, y)|}{1 + |\nabla f(x, y)|^2} \tag{15}$$

Direct application of (15) to real images is not practical owing to noise and strong texture variations. As in 1-D, (15) can be applied after smoothing the image, then computing partial derivatives or, by combining derivatives with the smoothing filter to produce the scaled index

$$\psi_\sigma[f(x,y)] = \frac{|g_\sigma(x,y) * f(x,y)||\nabla^2 g_\sigma(x,y) * f(x,y)|}{1 + |\nabla g_\sigma(x,y) * f(x,y)|^2}$$
(16)

The sensitivity of the index can be further improved by adopting a design mechanism inspired by Canny [4]. First, determine the direction along which the second order derivative of the isotropic gaussian filtered image attains a local maxima or minima, which is a good estimate of the direction orthogonal to an curvilinear singularity. Once this direction is estimated, evaluate the responses of the gaussian derivative filters along this direction and compute the ratio index as follows:

$$\psi[f(x,y)] = \frac{|f_{0,\theta,\sigma}(x,y) f_{2,\theta,\sigma}(x,y)|}{1 + |f_{1,\theta,\sigma}(x,y)|^2}$$
(17)

In (17), $f_{0,\theta,\sigma}(x,y)$, $f_{1,\theta,\sigma}(x,y)$, and $f_{2,\theta,\sigma}(x,y)$ are the responses to the zero, first and second order gaussian derivative filters along the direction specified by $\theta(x,y)$ and at a fixed scale σ. In particular, $f_{0,\theta,\sigma}(x,y)$ is just $f(x,y)$ smoothed by the gaussian function. The gaussian and the derivative filters used to compute (17) need not be isotropic. Elongated gaussians could be used to detect long curvilinear structures. However, to estimate the direction $\theta(x,y)$, we deploy an isotropic gaussian filter and exploit the steerable property of the second order gaussian directional derivative as described next.

Freeman and Adelson [11] showed that the response of a second order directional derivative of an isotropic gaussian can be synthesized as a linear combination of the responses of 3 second order derivatives along evenly spaced directions:

$$f * G_{2,\theta,\sigma} = 1/3(1 + 2\cos(2\theta))(J_{2,\theta=0,\sigma}) +$$
$$1/3(1 - \cos(2\theta) + \sqrt{3}\sin(2\theta))(J_{2,\theta=\pi/3,\sigma}) +$$
(18)
$$1/3(1 - \cos(2\theta) - \sqrt{3}\sin(2\theta))(J_{2,\theta=2\pi/3,\sigma})$$

In (18), $G_{2,\theta,\sigma}$ is the derivative of the isotropic gaussian along direction θ at a fixed scale σ, $\theta = 0, \pi/3, 2\pi/3$ are the basis directions, and $J_{2,\theta,\sigma}$ are the responses of the basis filters. Squaring the response (18) and expanding it results in a Fourier series in angle θ containing only even frequency terms. One can then use the lowest frequency terms to find the direction θ along which the squared second order directional derivative attains a local maximum or minimum [11]. Once this estimate of θ at each (x,y) is obtained, (17) can be applied to compute the singularity index. This approach is similar to Canny's method where the gradient orientation is first estimated and then non-maxima responses in the gradient direction are suppressed [4].

3. EXPERIMENTS

In all our experiments, we fixed the scale σ of the isotropic gaussian used to find the direction $\theta(x,y)$ to 2.2 pixels, and the constants $C_1 = 0$ and $C_2 = 1$. Prior to computing the singularity index (17), the local DC component was removed from each pixel by subtracting the local mean of pixel intensity values around the pixel. The local mean was computed using a unit-area isotropic gaussian of a large spatial width (σ = 15 pixels). This was done to locally debias the signal, eliminating asymmetric responses to discontinuities. We then computed the singularity index (17) by deploying elongated gaussians and their derivatives, where the major axis of the gaussian was elongated in the direction normal to $\theta(x,y)$. The scale σ of the elongated gaussian was set to 2.2 pixels and the aspect ratio (major axis to minor axis) was set to 2:1. The side-lobes in the singularity response of the second order directional derivative filters manifest as weak ringing artifacts. To ameliorate this problem, the scale σ at which the second order directional derivative response was computed was set to half the scale at which the first order directional derivative response was computed (σ = 2.2 pixels). This method produces stronger response to impulses, and better suppresses the already weak ringing artifacts.

Figs. 2, 3, and 4 illustrate the effect of applying the new singularity index defined in (17) to three real world images - a mammogram (Courtesy Emory University, Atlanta, GA, USA), a volcano on venus (NASA, Magellan Project/courtesy of apod.nasa.gov) captured by the Magellan spacecraft, and the Ganges river delta (NASA/courtesy of nasaimages.org) acquired as part of the NASA Human Spaceflight collection. The first column in the first row of each of these figures illustrates the original image, while the second column illustrates the output of the singularity index. The second row shows the result of applying non-maxima suppression (NMS) in the direction specified by $\theta(x,y)$. These results clearly illustrate a strong response by the singularity index to impulse-like structures, with suppressed response to edges.

4. FUTURE WORK

We presented a new singularity index for analyzing impulse singularities in images. Our analyses and experiments reveal a promising behavior by the index for detecting impulse-like or ridge curvilinear structures in images. The index is easily scalable using directional derivatives of gaussians. We plan to realize a multi-scale version of the index as part of future work. Also interesting is the fact that the reciprocal of the index is a powerful edge operator that rejects impulse singularities. We will explore this reciprocal index in future work as well.
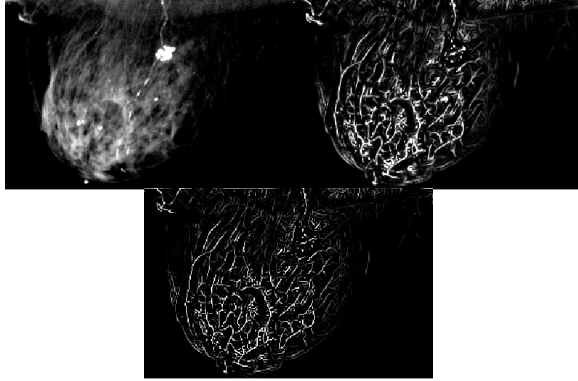
Fig. 2. Result of applying the singularity index (top right) defined in (17) to a mammogram (top left). The NMS result is shown below.
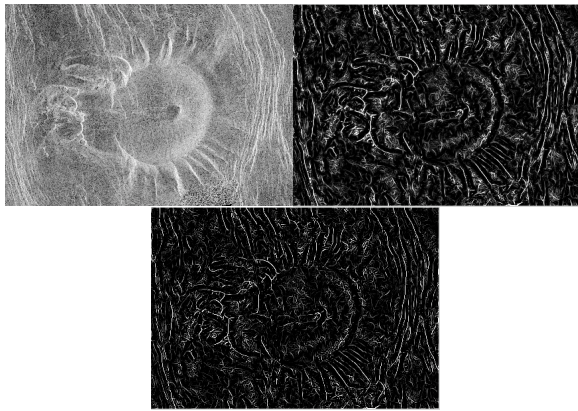

Fig. 3. Result of applying the singularity index (top right) defined in (17) to an image depicting a volcano on venus (top left). The NMS result is shown below.
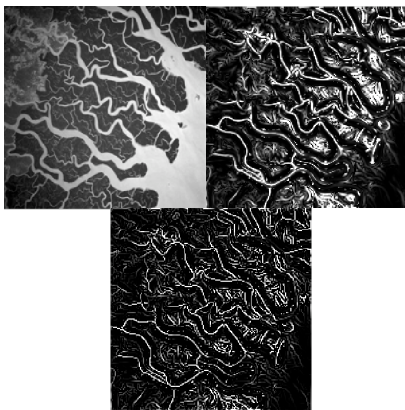

Fig. 4. Result of applying the singularity index (top right) defined in (17) to an image depicting the Ganges river delta (top left). The NMS result is shown below.

5. REFERENCES

[1] T. M. Koller, G. Gerig, G. Szekely, and D. Dettwiler, "Multiscale detection of curvilinear structures in 2-d and 3-d image data," in *IEEE Intl. Conf. Comput. Vision*. IEEE, 1995, pp. 864–869.

[2] L. G. Roberts, "Machine perception of three-dimensional solids," in *Optical and Electro-Optical Information Processing*. 1965, pp. 159–197, MIT Press.

[3] D. Marr and E Hildreth, "Theory of edge detection," *Proc. R. Soc. Lond. B 29*, vol. 207, no. 1167, pp. 187–217, 1980.

[4] J. Canny, "A computational approach to edge detection," *IEEE Trans. Pattern Anal. Mach. Intell.*, vol. 8, no. 6, pp. 679–698, 1986.

[5] S. Mallat and W. L. Hwang, "Singularity detection and processing with wavelets," *IEEE Trans. Inf. Theory*, vol. 38, no. 2, pp. 617–643, 1992.

[6] T. Lindeberg, "Edge detection and ridge detection with automatic scale selection," *Intl. J. Comput. Vision*, vol. 30, no. 2, pp. 117–154, 1998.

[7] C. Steger, "An unbiased detector of curvilinear structures," *IEEE Trans. Pattern Anal. Mach. Intell.*, vol. 20, no. 2, pp. 113–125, 1998.

[8] J. F. Kaiser, "Some useful properties of teager's energy operators," in *IEEE Intl. Conf. Acoust., Speech, and Signal Process.* IEEE, 1993, vol. 3, pp. 149–152.

[9] A. C. Bovik, P. Maragos, and T. F. Quatieri, "Am-fm energy detection and separation in noise using multiband energy operators," *IEEE Trans. Signal Process.*, vol. 41, no. 12, pp. 3245–3265, 1993.

[10] A. C. Bovik and P. Maragos, "Conditions for positivity of an energy operator," *IEEE Trans. Signal Process.*, vol. 42, no. 2, pp. 469–471, 1994.

[11] W. T. Freeman and E. H. Adelson, "The design and use of steerable filters," *IEEE Trans. Pattern Anal. Mach. Intell.*, vol. 13, no. 9, pp. 891–906, 1991.